FLOW-INDUCED VIBRATION OF A LARGE-DIAMETER ELBOW PIPING IN HIGH REYNOLDS NUMBER RANGE; RANDOM FORCE MEASUREMENT AND VIBRATION ANALYSIS

Kazuo Hirota, Yoshihide Ishitani, Tomomichi Nakamura, Tadashi Shiraishi, Hiromi Sago

Mitsubishi Heavy Industries Ltd, 2-1-1 Shinhama, Arai, Takasago, Hyogo, Japan

E-mail address of the corresponding author: kazuo_hirota@mhi.co.jp

Hidemasa Yamano, Shoji Kotake

Japan Atomic Energy Agency, 4002 Narita, O-arai, Ibaraki, Japan

ABSTRACT

The design of Japanese large-scale sodium-cooled fast reactor requires increase in primary coolant velocity and enlarging the diameter of piping, so that a flow-induced vibration for this piping with a short radius elbow should be considered. To evaluate this vibration, flow-induced-vibration tests have been carried out using two kinds of 1/3-scale elbow test sections, which simulate a hot-leg piping. In the flow visualization test using the test section made of acrylic resin, pressure fluctuations and correlation lengths have been obtained with pressure sensors. In the flow-induced-vibration test using the test section made of stainless steel, natural frequencies, mode and random vibration response have been measured. Random vibration stress on the test section has been calculated from the power spectrum densities of pressure fluctuations and their correlation lengths by a vibration analysis method based on random vibration theory. This method has been verified by comparison with the vibration stress obtained from the flow-induced-vibration test.

1. INTRODUCTION

An innovative two-loop primary cooling system is adopted in a Japanese large-scale sodium-cooled fast reactor (JSFR) in the conceptual design stage, as shown in Figure 1. This primary cooling system increases the primary coolant flow rate per loop. As a result, a large-diameter piping system with remarkably high coolant velocity is required. The piping thickness in the JSFR is designed to be considerably thinner than that in light water reactors. The JSFR has only one L-shaped elbow for the hot-leg piping system and three elbows for the cold-leg one. The curvature of the elbow is equivalent to the piping diameter for the compact system design. Based on these features, the flow dynamics and flow induced vibration behavior in the piping with elbow should be investigated to ensure feasibility of the JSFR cooling system design.

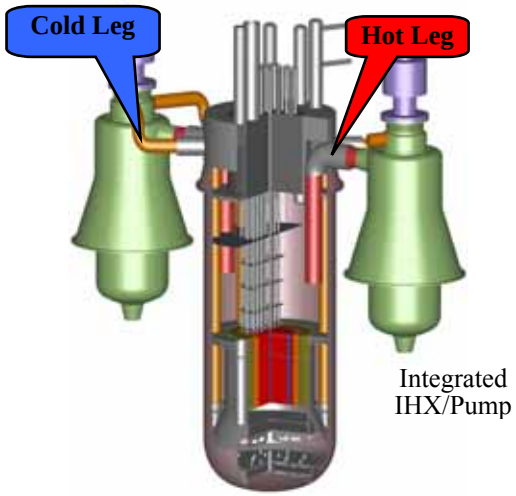

Figure 1: *Configuration of Primary Cooling System*

For that purpose, a flow visualization test with water has been performed under room temperature (Nakamura et al. 2005). In the test, pressure fluctuations have been measured to obtain power spectrum densities (PSDs) and correlation lengths for vibration response evaluation.

The objectives of this paper are, to investigate the effect of coolant viscosity on the fluid forces, to measure random-vibration of the piping, and to verify the flow-induced-vibration analysis method. For the first objective, the flow visualization test has been carried out under 60°C in order to compare the experimental data under room temperature. The measured random vibration has been provided to the verification data for the vibration analysis method.

2. TEST FACILITY

The outline of the water test loop is shown in Figure 2. The elbow test section is installed on the upper part of the rectification tank, which corresponds to the reactor vessel. The piping diameter is 0.41m, which is 1/3 scale of that of the JFSR's hot-leg piping.

Two types of test sections have been prepared. One has been made of acrylic resin for "flow visualization test" to investigate the flow pattern and pressure fluctuation. The other has been made of stainless steel for "flow-induced-vibration test" to obtain vibration characteristics and flow-induced-vibration response. In the latter test, the stiffness and support conditions of the test section agree with the JFSR's hot-leg piping conditions. To well observe flow dynamics in the flow visualization test, the upward straight part of the pipe has been installed on the rectification tank as shown in Figure 3.

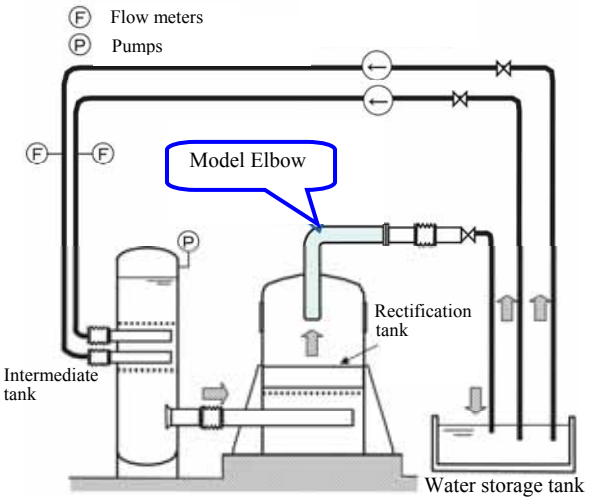

Figure 2: *Outline of Test Facility*

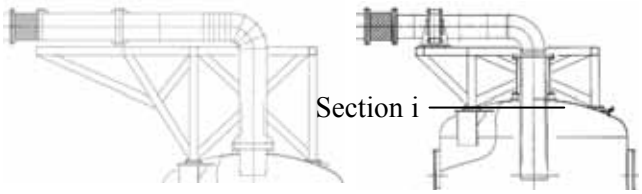

(*Flow visualization test*) (*Flow induced vibration test*)

Figure 3: *Test sections of Flow Visualization Test and Flow Induced Vibration Test*

3. TEST RESULTS

3.1 Pressure fluctuation

According to the flow visualization results, the flow in the elbow separates from the inner surface at around 67° of the elbow angle, then it reattaches at about 290mm down stream from the separation point (Shiraishi et al. 2006). The test results under 60°C are similar to those under room temperature.

The pressure fluctuations have been measured with 124 pressure sensors fixed at 18 different cross sections along the piping shown in Figure 4 in order to estimate fluctuating fluid force acting on the pipe. The test conditions were set maximum 9.2m/s (designed value) as mean velocity under 60°C, which gives 8×10^6 of Reynolds number: around 1/5 of the JSFR hot-leg condition.

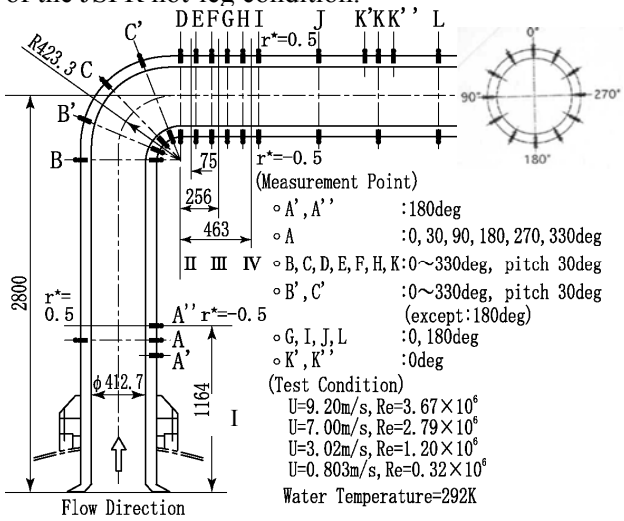

Figure 4: *Location of Pressure Sensors*

Figure 5 shows PSDs of the measured pressure fluctuations at 9.2 m/s under 60°. Figure 5(a) shows the data measured in the outside of the elbow (0° of angular position). Figure 5(b) shows the inside of the elbow (150°), which corresponds to the boundary of the flow separation region. Figure 5(a) shows flat spectral shape, whereas Figure 5(b) shows a peak at 10Hz.

Figure 6 shows non-dimensional PSDs of pressure fluctuations plotted versus the reduced frequency St; These dimensionless quantities are defined as follows.

$$St = fD/U, \qquad P(f) = P_{measured}(f)/(1/2)^2 \rho^2 U^3 D \qquad (1).$$

Non-dimensional frequency is Strouhal number. The PSDs of the pressure fluctuation P(f) divided by square of dynamic pressure and D/U derives the non-dimensional PSDs. The flow in the separation region fluctuates periodically in the horizontal direction, perpendicular to the pipe axis. The non-dimensional peak frequency of the flow fluctuations is around 0.45.

The non-dimensional PSDs of pressure fluctuations under 60°C are in good agreement with those under room temperature. Pressure fluctuation data have been measured under some flow velocity conditions as one of parameters. The non-dimensional PSDs of pressure fluctuations are independent of the flow velocity as well.

The present flow visualization tests have indicated that the effect of coolant viscosity on pressure fluctuations is very small.

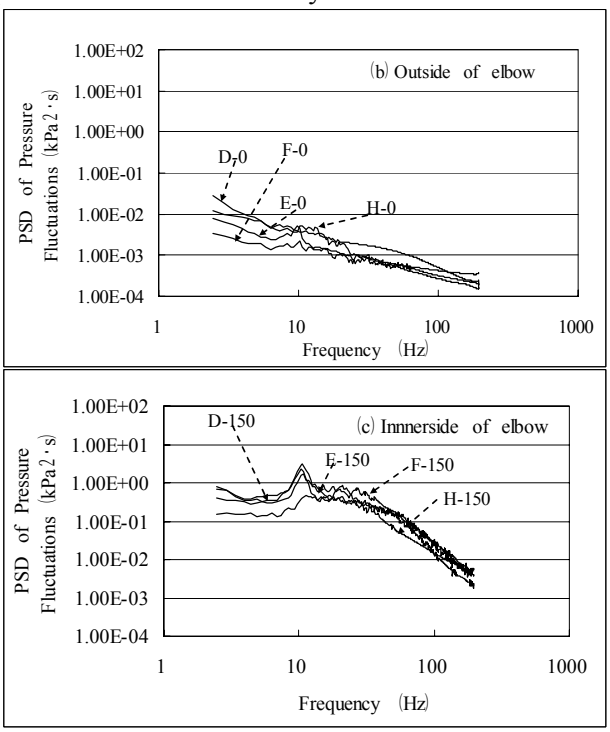

Figure 5: *Power spectrum densities of pressure fluctuation*

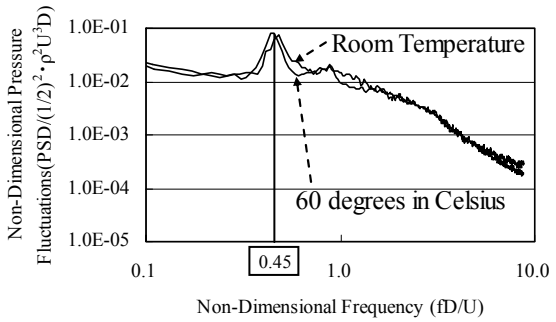

Figure 6: *Non-dimensional PSD (9.2m/s)*

3.2 Correlation length

As proposed by Au-Yang (1980), the real part of the cross spectrum between two locations is used to derive the axial and circumferential correlation length λ_c, λ_a:

[Axial direction]

$$\mathrm{Re}\left(\Gamma_{ss'}\right) = \exp\left(-\left|s-s'\right|/\lambda_a\right)\cos\left(2\pi f\left|s-s'\right|/U\right) \quad (2)$$

$$\lambda_a = \frac{-\left|s-s'\right|}{In\left(\Gamma_0\right) - f/f_0} \quad (3).$$

[Circumferential direction]

$$\mathrm{Re}\left(\Gamma_{rr'}\right) = \exp\left(-\left|r-r'\right|/\lambda_c\right) \quad (4).$$

$$\lambda_c = \frac{-\left|r-r'\right|}{In\left(\Gamma_0\right) - f/f_0} \quad (5).$$

Here, Γ_0 means the real part of the coherence at zero frequency, and f_0 is the frequency where the magnitude of coherence becomes 1/e. Each pair of measured pressure fluctuations at two different locations is fitted by using the above equations from eqs. (2) to (5) to derive the correlation lengths λ_c, λ_a.

Figure 7 shows the estimated axial and the circumferential correlation length λ_a and λ_c at U=9.2 m/s. There is little correlation on the data from the cross section A to B. The maximum correlation length in the elbow is observed at the inner side (180°) of the elbow.

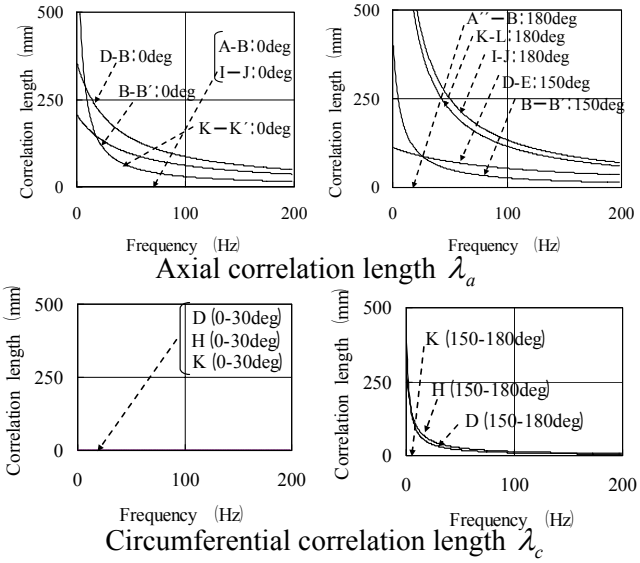

Figure 7: *Correlation Length*

3.3 Vibration characteristics of the test section for flow induced vibration

In the JSFR design, the hot-leg piping is surrounded by a support pipe, which is intended to retain leaked coolant assuming the pipe break. Such a piping configuration has been simulated to obtain the vibration characteristics in the flow-induced-vibration test. In the test, 12 accelerometers for beam mode and 16 for shell mode were installed on the test section. Prior to the flow-induced-vibration test, impact testing was executed to obtain the vibration characteristics. The elbow part of the test section was excited by an impact hammer with a force transducer. From the impact testing, natural frequencies and damping ratios were obtained as shown in Table 1. Their mode shapes were also obtained from transfer function between impact force and acceleration.

Figure 8 shows natural frequencies and their mode shape. The beam type modes were observed at 23.0Hz and 28.5Hz. The shell type modes were also observed; the same phase mode of the hot leg and support pipe (59.0Hz) and the opposite phase mode (73.0Hz).

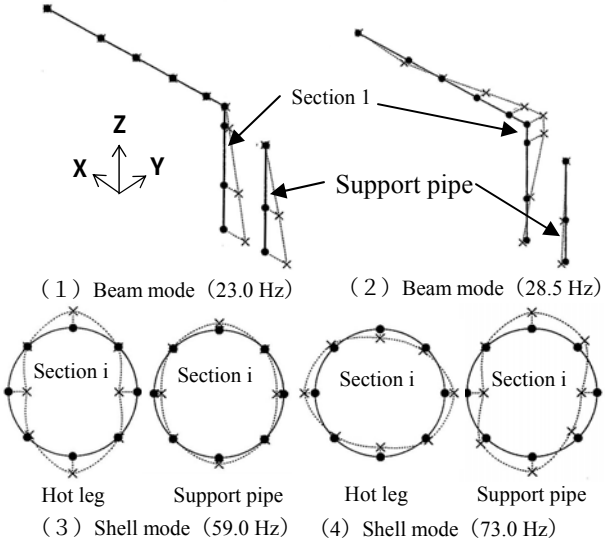

Figure 8: *Natural frequency and mode shape*

	In air		In water	
Natural mode shape	F(Hz)	ζ(%)	F(Hz)	ζ(%)
1st beam mode (X direction)	39.0	0.81	23.0	1.06
1st beam mode (Y direction)	53.0	0.48	28.5	1.66
2nd Shell mode (In-phase)	102.0	0.23	59.0	0.38
2nd Shell mode (Out of phase)	132.0	0.19	75.5	0.53
2nd Shell mode (Only hotleg)	179.5	0.26	105.0	0.41
3rd Shell mode (0 deg. direct.)			135.5	0.36
3rd Shell mode (90 deg. direct.)			149.0	0.32
3rd Shell mode (Only hotleg)			158.0	0.38
2nd beam + 2nd Shell mode			186.0	0.34

Table 1: *Natural frequencies and mode shape*

3.4 Flow induced vibration test

Flow induced vibration response has been measured with some strain gauges installed at some locations where vibration stress was expected to be large. Figure 9 shows frequency spectra of the vibration stress under room temperature at flow velocity 9.2m/s. Not only beam type modes but also shell type modes were observed because of the thin thickness of the pipe. No vibration was observed at 10Hz which corresponds to the frequency of fluctuating pressure near flow separation region at the elbow. This is because the region with periodical fluctuating pressure is small compared to flow area in the hot-leg piping and the excitation direction induced by the flow separation is z direction in which stiffness of the pipe is high.

The obtained experimental data is provided to the verification of the random vibration analysis method mentioned afterwards.

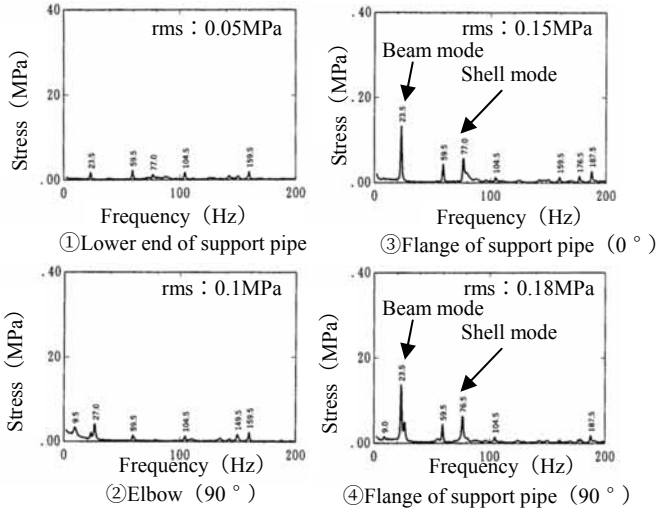

Figure 9: *Random Vibration Stress*

4. VIBRATION ANALYSYS

4.1 Analysis results of vibration characteristics

Vibration characteristics were analyzed by finite element method code FINAS, which can consider a fluid-structure coupling effect. Figure 10 shows the analysis model of the test equipment. The rectification tank and the support are considered to simulate the boundary condition of the test section.

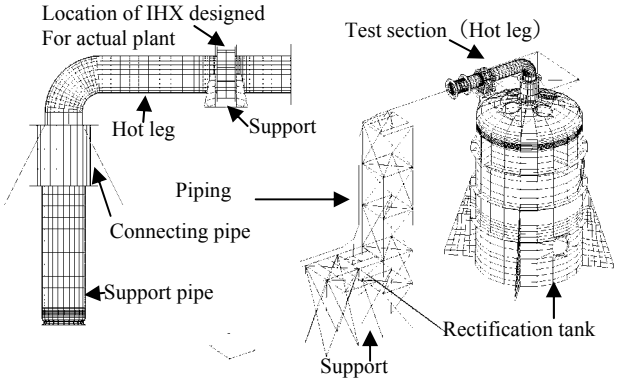

Figure 10: *Analysis Model of Test Equipment*

Figure 11 shows the analysis results of natural frequency and mode shape with water inside the pipe. Analysis results of natural frequency and mode shape show good agreement with those of vibration test results in Figure 8.

4.2 Random vibration analysis method

The random vibration response of the pipe can be calculated by random vibration theory using PSDs of pressure fluctuations and correlation lengths. The root-mean-square of displacement $\bar{y}(s)$ at the location s is expressed as follows by using the

natural mode $\phi_j(s)$, transfer function $H_j(\omega)$ and the statistical excitation force $L_j(\omega)$.

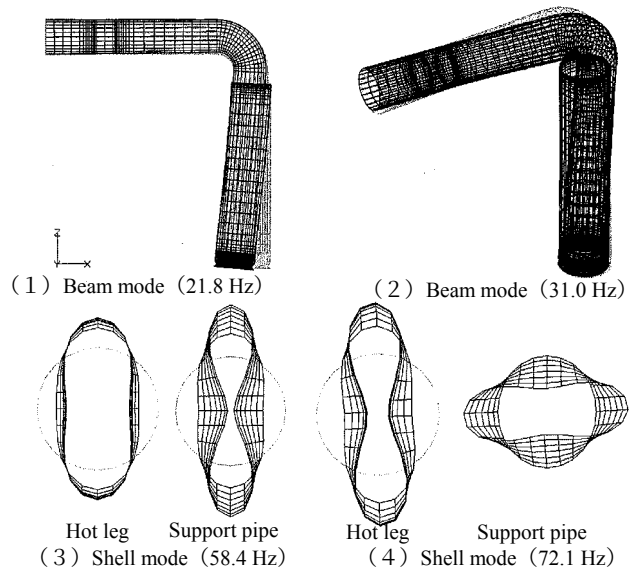

Figure11: *Natural frequency and mode shape*

$$\overline{y}^2(s)=\sum_{j=1}^{n}\phi_j{}^2(s)\int_0^{\infty}L_j(\omega)\left|H_j(\omega)\right|^2 d\omega \qquad (6).$$

$H_j(\omega)$ and $L_j(\omega)$ are expressed as follows.

$$H_j(\omega)=\left[\left(1-\frac{\omega^2}{\omega_j^{\,2}}\right)+2ih_j\frac{\omega}{\omega_j}\right]^{-1} \qquad (7).$$

$$L_j(\omega)=\frac{1}{M_j{}^2\omega_j{}^2}\iint_{Surface}R(s,s',\omega)\phi_j(s)\phi_j(s')dsds' \qquad (8).$$

$$M_j=\int_{Surface}m(s)\phi_j{}^2(s)dS \qquad (9).$$

$$R(s,s',\omega)=\frac{1}{\pi}P(s,\omega)\tilde{R}_{ss'}{}^2(\omega)\cos\theta_{ss'}(\omega) \qquad (10).$$

In Eq. (10), $P(s,\omega)$ is the auto-correlation of pressure fluctuations on the inner surface of the pipe, and $\tilde{R}_{ss'}{}^2(\omega)\cos\theta_{ss'}(\omega)$ is approximated by the following cross spectral function proposed by Au-Yang (1980),

$$\Gamma_{ss'}(\omega)=\exp\left(-\frac{l}{\lambda_c}\right)\exp\left(-\frac{L}{\lambda_a}\right)\exp\left(i\omega\frac{L}{U}\right) \qquad (11).$$

l and L express the distances between two locations in the circumferential and the axial direction of the pipe, respectively. λ_c,λ_a express the correlation lengths corresponding to those two directions.

The pressure fluctuations can be produced with the vortices conveyed by the turbulent flow. The correlation in the circumferential direction corresponds to the first term of the right hand side of Eq. (11), while the correlation in the axial direction consists of the remaining two terms, which include the convection component by the flow velocity U.

Figure 12 shows the PSDs of pressure fluctuation used for turbulence induced vibration analysis. It is very time-consuming to input detailed pressure distribution as excitation force into analysis model. Therefore average PSDs of pressure fluctuation in some sections were input to the corresponding section in the analysis model. The pressure fluctuation of the flow separation region of the elbow is apparently large compared with the other regions. Then the downstream region of the inner side of the elbow can be divided into two regions, large pressure fluctuation region of the inner side (90° - 180° - 270°) of the elbow and the other angular region. The test section is divided into five regions with reference to the PSD distribution of pressure fluctuation. The lines of Figure 12 are average PSD in the respective regions.

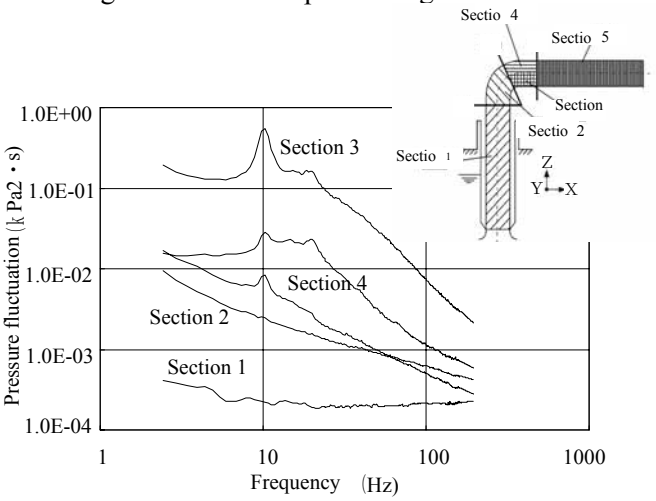

Figure 12: *Average PSDs of Pressure Fluctuation for Random Vibration Analysis*

Figure 13 and 14 show the correlation lengths in the axial and the circumferential direction used for vibration analysis. The correlation length has also been grouped to several regions, in each of which correlation lengths are averaged. Taking into account characteristics of the correlation length distributions, the correlation lengths can be summarized in some regions. Therefore the regions of the test section for the correlation lengths are fewer than those for the PSDs. The lines in Figures 13 and 14 are average correlation lengths in the respective regions.

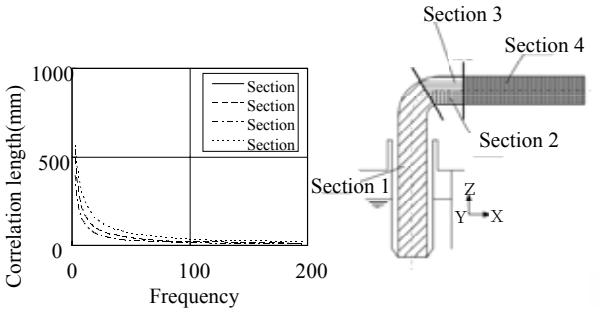

Figure 13: *Axial Correlation Length Used for Random Vibration Analysis*

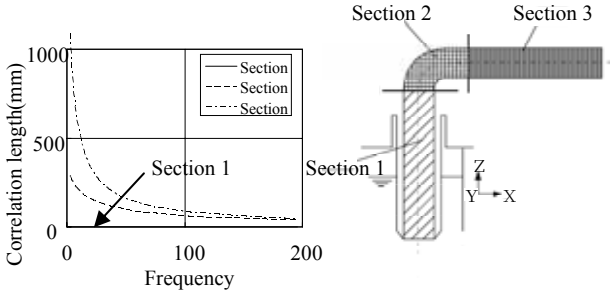

Figure 14: *Circumferential Correlation Length Used for Random Vibration Analysis*

4.3 Random vibration analysis results

Figure 15 shows calculated frequency spectra of the vibration stress at the same locations as the stress measurement. The analysis condition is the vibration under room temperature at flow velocity 9.2m/s. Not only beam type modes but also shell type modes appear as measured by flow induced vibration test. No vibration was observed at 10Hz which corresponds to periodical pressure fluctuation in the flow separation region.

Figures 9 and 15 contain the root mean square of measured and calculated vibration stress, respectively. The ratio of the analysis results to the test results is from 1.0 to 2.0. Therefore it is concluded that the vibration analysis method is valid to evaluate the vibration stress of the JFSR's hot leg piping reasonably.

The reason why the analysis results are larger than the test ones is considered to be the following. The dominant mode of the vibration stress of the pipe is the first natural mode for which the pipe vibrates at the lower part of the hot leg and support pipe. The vibration level of the first mode strongly depends on the PSD and correlation length in the lower part of the hot leg piping, which corresponds to the section 1 in Figures 12, 13 and 14. The correlation length in this part is very short as shown in Figures 13 and 14. However the vibration analysis method cannot consider the correlation length less than the element size of the analysis model. The method applies 100% coherent in the element. We will improve the analysis method in order to consider correlation length less than element size of the analysis model.

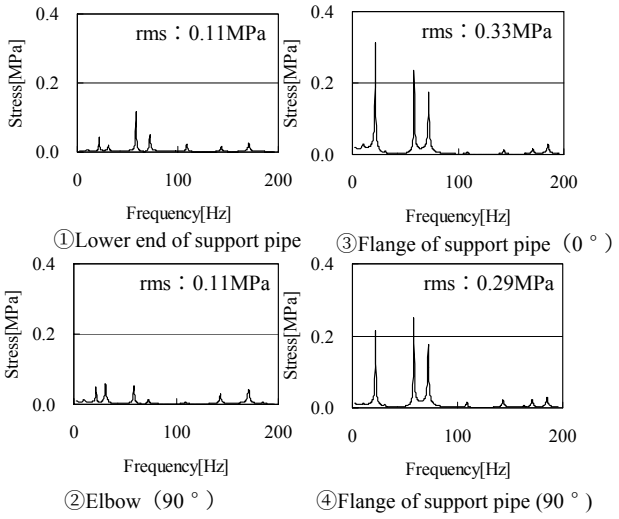

Figure 15: *Calculated Random Vibration Stress*

5. CONCLUSION

The flow induced vibration test using a 1/3 scale test section simulating a hot leg piping of the JFSR has been conducted. Compared to the previous test under room temperature, the flow visualization test has indicated that the effect of coolant viscosity on the pressure fluctuations is very small. The flow-induced vibration test revealed that the periodical pressure fluctuation near the flow separation region does not significantly affect the vibration of the hot leg piping. The random vibration analysis method has been verified using the experimental data. Therefore the vibration analysis method can evaluate the vibration stress of JFSR's hot leg piping reasonably.

6. REFERENCES

Au-Yang,M.K., 1980, Dynamic Pressure inside a PWR – A Study based on Laboratory and Field Test Data, *Nuclear Engineering and Design*, Vol.58, pp.113-125.

T. Nakamura et al., 2005, "Flow-induced Vibration of a Large-diameter Elbow Piping based on Random Force Measurement caused by Conveying Fluid," *Proc. of ASME PVP Conf.*, PVP2005-71277.

T. Shiraishi et al., 2006, "Resistance and Fluctuating Pressures of a Large Elbow in High Reynolds Numbers," *Journal of Fluids Engineering*, 128, 1063-1073.